Preprints.org

Communication

Not peer-reviewed version

HABS-controlled Growth of Aragonite Based Polymorphic Symbiotic CaCO3 Crystals in Emulsion

Weiwei He , Junqing Hu , Weihao Sun , Jiqiong Liu , Hongguang Guo , Changming Zhao , Qinggguo Wang , Xiangbin Liu , Meng Cai , Weiguang Shi *

Posted Date: 25 April 2023

doi: 10.20944/preprints202304.0888.v1

Keywords: aragonite; HABS; symbiotic crystals; superstructure; mineralization; kerosene emulsion

Preprints.org is a free multidiscipline platform providing preprint service that is dedicated to making early versions of research outputs permanently available and citable. Preprints posted at Preprints.org appear in Web of Science, Crossref, Google Scholar, Scilit, Europe PMC.

Copyright: This is an open access article distributed under the Creative Commons Attribution License which permits unrestricted use, distribution, and reproduction in any medium, provided the original work is properly cited.

Preprints (www.preprints.org) | NOT PEER-REVIEWED | Posted: 25 April 2023 doi:10.20944/preprints202304.0888.v1

Disclaimer/Publisher's Note: The statements, opinions, and data contained in all publications are solely those of the individual author(s) and contributor(s) and not of MDPI and/or the editor(s). MDPI and/or the editor(s) disclaim responsibility for any injury to people or property resulting from any ideas, methods, instructions, or products referred to in the content.

Communication

HABS-Controlled Growth of Aragonite Based Polymorphic Symbiotic $CaCO_3$ Crystals in Emulsion

Weiwei He [1], Junqing Hu [2], Weihao Sun [2], Jiqiong Liu [3], Hongguang Guo [3],Changming Zhao [3], Qingguo Wang [3], Xiangbin Liu [3,4], Meng Cai [3] and Weiguang Shi [4,5,*]

[1] School of Mechatronic Engineering, Daqing Normal University, Daqing 163712, China
[2] No.2 oil production factory of Daqing Oilfield Ltd., Daqing 163414, China
[3] Oil Production Engineering Research Institute of Daqing Oilfield Ltd., Daqing 163453, China
[4] College of Chemistry & Chemical Engineering, Northeast Petroleum University, Daqing 163318, China
[5] Key Laboratory of Continental Shale Hydrocarbon Accumulation and Efficient Development, Ministry of Education, Northeast Petroleum University, Daqing 163318, China
* Correspondence: sswwgg2003@126.com

Abstract: Non-natural mineralization of $CaCO_3$ with special structures or morphology is generated during the crude oil migration, which is the main scale of alkaline/surfactant/polymer (ASP) flooding in oilfields, adversely affecting the oil recovery and causing environmental pollution. Up to now, the mineralization of superstructural symbiotic aragonites and the role of heavy alkyl-benzene sulfonate (HABS) in directing mineralization are still unclear. In this work, rosette-like, bouquet-like and dumbbell-like aragonite-based superstructure of symbiotic $CaCO_3$ crystals were obtained in a simulated O/W emulsion with HABS, which can help understanding the diversified growth of $CaCO_3$ scaling in oilfield. As a result, HABS stabilized micelles acted as a framework for mineralization, and promoted the accumulation of Ca^{2+} and CO_3^{2-}, generating pre-nucleation clusters and partial ion pairs by electrostatic attraction. Following, the sequential nucleation of amorphous $CaCO_3$ interconnected with HABS molecules. Finally, these nanoparticles transformed into micro-meter crystals via dissolution-reprecipitation, forming the superstructures that controlled by a synergistic effect between HABS and kerosene phase. This work may enrich the understanding of $CaCO_3$ mineralization in oilfield, provide theoretical support for the prevention of hard carbonate scaling, and also provide a novel strategy for organic-inorganic composites manufacturing.

Keywords: aragonite; HABS; symbiotic crystals; superstructure; mineralization; kerosene emulsion

1. Introduction

As the most abundant minerals in the world, $CaCO_3$ has attracted tremendous attention due to its multitudinous morphologies and polymorphs [1–4]. To date, studies have shown that $CaCO_3$ has seven phases, including amorphous calcium carbonate (ACC) [5], calcium carbonate monohydrate (monohydrocalcite) [6], calcium carbonate hexahydrate [7], rhombohedral calcite [8], orthorhombic aragonite [9], and hexagonal vaterite [10], as well as the newly discovered phase calcium carbonate hemihydrate [11]. In addition, $CaCO_3$ or $CaCO_3$-based materials processes significant applications, especially in bone regeneration and drug delivery due to its excellent biocompatibility [12,13]. However, $CaCO_3$ can exist in different morphologies and crystal structures, some of them might serve as scaling to reduce the oil recovery. Also, the scaling phenomenon is common in industrial production processes, such as circulating cooling water systems, and pipe flow systems [14]. And the details of these scaling processes and the exact role played by polymorphic $CaCO_3$ have not been identified.

Aragonite, as a high-temperature metastable polymorph of $CaCO_3$, usually exists in the form of a needle-like crystals, which is the main constituent in many sea shells and corals, and can also form

© 2023 by the author(s). Distributed under a Creative Commons CC BY license.

Preprints (www.preprints.org) | NOT PEER-REVIEWED | Posted: 25 April 2023 doi:10.20944/preprints202304.0888.v1

inorganically in warm shallow seas [15]. Besides, aragonite is also an ideal reinforcement composite materials due to its strange orientation important biomineral [16]. And for this purpose, selectively control the formation of this material is around the corner. Hence, a number of approaches have been widely made to control the morphology of aragonite crystals, such as nanofilament network [17], tablet-like [18], needle-like and dandelion-like superstructures [19,20]. Furthermore, although aragonite exhibits various morphologies, the dumbbell-like superstructure was rarely reported. In our previous research, labyrinth-like calcite crystals were synthesized in HPAM–HABS hybrid system (HPAM: partially hydrolyzed polyacrylamide; HABS: heavy alkylbenzene sulfonate, two main constituents in ASP flooding in oil fields) [21]. However, the regulating effect of HABS in the formation of aragonite and symbiotic mixed $CaCO_3$ crystals in emulsion system is still unclear. Compared to water phase, oil/water interfaces provide a unique non-equilibrium reaction environment with high surface energy and determine the transporting behavior of ions and/or atoms across the outer surroundings. This leads to synthesize novel structural nanomaterials via complex crystallization processes, and further our knowledge about $CaCO_3$ oil scales.

Herein, we reported a simple synthesis method of symbiotic mixed aragonite with special morphology by applying the "one-step precipitation method" in 20 V% O/W HABS/kerosene emulsion. Our research may provide a HABS-stabilized interface for the orientation growth of $CaCO_3$ crystals and a simulated environment of the crude oil migration, and offer a successful remediation strategy to deal with carbonate scale in oilfield.

2. Materials and Methods

2.1. Materials

Calcium chloride ($CaCl_2$, AR grade), sodium carbonate ($NaCO_3$, AR grade) were purchased from Tianjin chemical reagent factory. Heavy alkyl-benzene sulfonate (HABS, average molecular weight: 400-430) was obtained from Daqing Donghao Investment Co. Ltd. Kerosene purchased from Shanghai Aladdin biochemical technology co., LTD is used as the oil phase, of which the purity exceeds 99%. All above reagents were obtained from commercial sources and received without further purification. Deionized water was used to prepare aqueous solutions of $CaCl_2$ and $NaCO_3$ just before crystallization experiment, which was made in our laboratory.

2.2. Preparation of $CaCO_3$ crystals

Aqueous solution of $CaCl_2$ (0.04mol/L, 250mL), aqueous solution of $NaCO_3$ (0.04mol/L, 250mL), a certain concentration of HABS were prepared beforehand. Calcium carbonate products were precipitated by the method of quickly pouring 25mL aqueous solution of $NaCO_3$ and a certain concentration of HABS into 200mL beaker containing a fixed volume content of kerosene (20 v%) with 25mL $CaCl_2$ solution, and corresponding distilled water with various volume content (total volume: 100ml).), then rapid stirring for 10 minutes (10000 rpm) and agitated with a magnetic stirrer (300 rpm) for 1 hour providing different reaction conditions. The HABS controlled kerosene emulsion is O/W type emulsion. The resulting precipitates were filtered and washed thoroughly with distilled water. Finally, the product was dried in the oven at 45 °C for 24 hours and used for further measurements.

The effects of reaction conditions on crystals are including temperature (35 °C, 45 °C, 55 °C, 65 °C, 75 °C, and 85 °C), reaction time (5mins, 10mins, 20mins, 30mins, and 60mins) , and the concentration of HABS (200mg/L, 400mg/L, 600mg/L, 800mg/L, and 1000mg/L).

2.3. Calculation method of relative fraction of aragonite, vaterite and calcite

The relative mole fraction of vaterite and calcite were calculated from their characteristic pXRD peak intensities by the following equation [22]:

$$x_V = 7.691 \frac{I_V^{110}}{I_C^{104} + 7.691(I_V^{110}) + 3.157(I_A^{221})} \quad (1)$$

Preprints (www.preprints.org) | NOT PEER-REVIEWED | Posted: 25 April 2023 doi:10.20944/preprints202304.0888.v1

$$X_V + X_A + X_C = 1 \quad (2)$$

$$\frac{I_C^{104}}{I_V^{110}} = 7.691\frac{X_C}{X_V} \quad (3)$$

$$X_V + X_C = 1 \quad (4)$$

$$\frac{I_C^{104}}{I_A^{221}} = 3.157\frac{X_C}{X_A} \quad (5)$$

$$X_A + X_C = 1 \quad (6)$$

Where, X_A is the mole fraction of vaterite, X_V is the mole fraction of vaterite, and X_C is calcite. I_C 104, I_A 221and I_V 110 are the pXRD intensities of the {104} planes, {221} planes and {110} planes represent calcite, aragonite and vaterite, respectively.

3. Results and Discussion

A simulated mineralization approach is designed by mixing HABS/Na_2CO_3 solution and $CaCl_2$/kerosene emulsion (20 V% O/W) to prepare the symbiotic mixed aragonite crystals. It can be clearly seen in Figure 1, $CaCO_3$ crystals present bouquet-like and dumbbell-like morphologies with radiated bundles. A key question is how crystals of vaterite-aragonite, aragonite and calcite-aragonite can be molded into such convoluted. Aiming at studying the crystallization process of $CaCO_3$ in HABS-controlled kerosene emulsion system, a series of $CaCO_3$ precipitates were synthesized through changing the concentration of HABS, reaction temperature and time, being listed in Tables S1–S3.

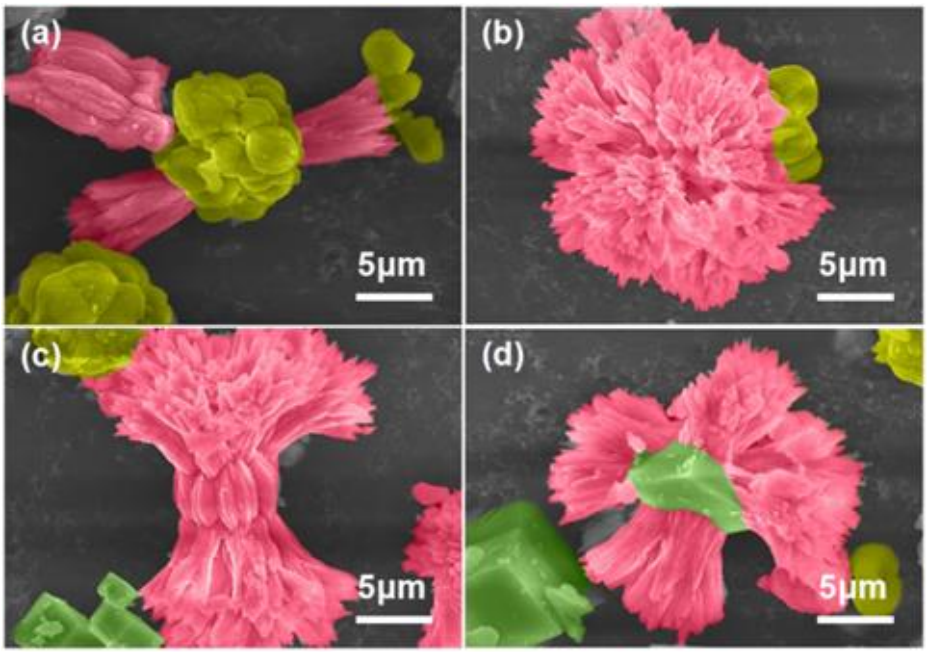

Figure 1. SEM images of $CaCO_3$ crystals in HABS-controlled kerosene emulsion.

3.1. Effects of HABS on the polymorphic symbiotic $CaCO_3$ crystals

Aiming at investigating the effect of concentration of HABS on the polymorph and morphology of $CaCO_3$ products in kerosene emulsions, experiments were carried out at 45 °C for 1h with different HABS concentrations. Simultaneously, the corresponding $CaCO_3$ crystals were characterized by SEM, FTIR and XRD. Figure 2a–e shows the morphologies evolution of $CaCO_3$ under different HABS concentration. It is obvious that rosette-like, dumbbell-shaped and cubic crystals obtained with a wide size distribution from 5 to 10μm in the lower concentration of HABS (200mg/L, 400mg/L,

Preprints (www.preprints.org) | NOT PEER-REVIEWED | Posted: 25 April 2023 doi:10.20944/preprints202304.0888.v1

600mg/L), especially at 200mg/L. Whereas, further increasing the HABS concentration to 800mg/L and 1000mg/L, the spherical vaterite products were in the majority. We can speculate that vaterite nuclei on the HABS surfaces by lowering the activation energy of nucleation (ΔG) through interfacial recognition, thus make kinetic control of vaterite possible [22]. On the basis of this, the increasing interaction of sulfonate groups of HABS and Ca^{2+} could gradually induce the formation of less stable vaterite crystals. These spherical structures aggregated with many nano-sized particles, showing rough surfaces (Figure S1). It is likely these vaterite particles were assembled by lots of amorphous phase and then transformed to calcite via a "dissolution-reprecipitation mechanism" [23].

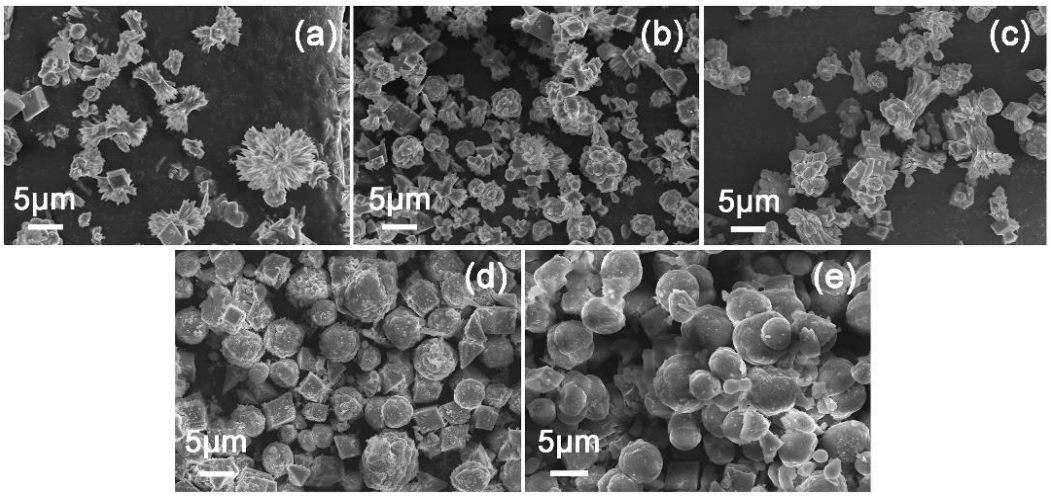

Figure 2. Morphologies of $CaCO_3$ under various HABS concentration ((**a**) 200mg/L; (**b**) 400mg/L; (**c**) 600mg/L; (**d**) 800mg/L; (**e**) 1000mg/L).

Generally, there four main FTIR adsorption bands of C-O bond vibrations with regard to $CaCO_3$, containing symmetric stretching (υ1), out-of-plane bending (υ2), asymmetric stretching (υ3) and in-plane bending (υ4) [24,25]. According to the FTIR results (Figure 3a), four characteristic peaks were found at 1471cm^{-1}, 1083cm^{-1}, 876/856cm^{-1}, 745/713cm^{-1} in the lower concentration (200mg/L, 400mg/L, 600mg/L), indicating that these precipitates were the mixed phase of calcite, aragonite, vaterite and ACC transformed into more of $CaCO_3$ polymorphs [26]. With the increase of HABS concentration, the tendency to form vaterite went up, indicating a strong stabilization of vaterite phase by high HABS concentration. Especially when the HABS concentration was greater than 800mg/L, obtaining a mixture phase of vaterite and partial calcite (875cm^{-1}, 745/713cm^{-1}), without aragonite being found.

The pXRD analysis of the prepared particles was also performed to gain information on the structure changes of those products, revealing that it underwent a polymorph evolution process. Precisely, the pXRD patterns in the lower concentration (200mg/L, 400mg/L, 600mg/L) in Figure 3b at (2θ) 29.4°, 24.9°, 27°, 32.8°, 36.2°, 41.2° can be assigned to the (104), (110), (112), (114), (220) and (221) crystalline planes of calcite, vaterite and aragonite, respectively [27]. When HABS concentration increased to 800mg/L and 1000mg/L, the reflections of aragonite disappeared and vaterite became dominant. Importantly, the polymorphs of these samples are consistent with FTIR patterns. Calculations of polymorphic ratios, the content of vaterite, calcite and aragonite were shown in Figure 3c [28]. Notably, calcite experienced a fluctuation at about 40% as HABS concentration varied. With the increase of HABS concentration, the tendency to form aragonite declined from 30% at 200mg/L to 0 at 800mg/L. Interestingly, the content of vaterite progressively dominated, indicating that the higher HABS concentration (>600mg/L) exerted a strong stabilization role on vaterite.

Preprints (www.preprints.org) | NOT PEER-REVIEWED | Posted: 25 April 2023 doi:10.20944/preprints202304.0888.v1

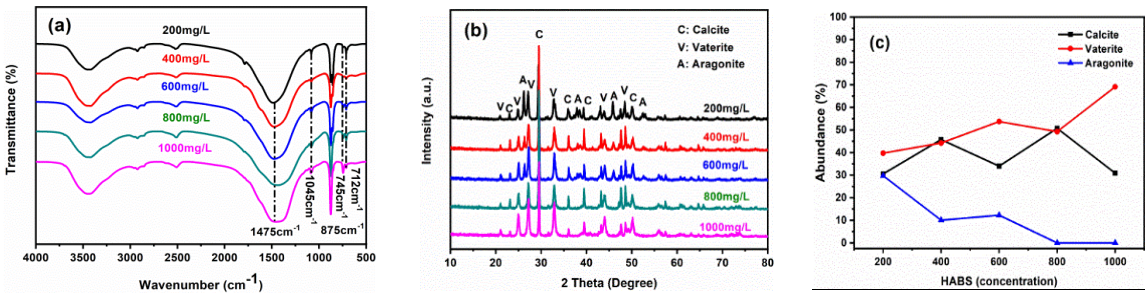

Figure 3. FTIR, XRD and content variation of CaCO3 crystals under various HABS concentration.

3.2. Effects of reaction time and temperature on the polymorphic symbiotic $CaCO_3$ crystals

To further investigate the growth mechanism, time-resolved experiments were performed in a 600mg/L HABS solution at 45 °C. Figure 4 showed the SEM images of $CaCO_3$ products generated of temporal evolution. Obviously, before 20 mins crystallization, many highly aggregated particles with several micrometres of $CaCO_3$ emerged (Figure 4a–c). The coalescence behaviour of the rounded crystals indicates the that in the initial stage, the presence of ACC on the oil/water interface promoted the aggregation of ACC-stabilized oil droplets, thus leading the formation of larger particles in the growth stage [29]. Branching needles and cubic bulks were obtained after 30 mins crystallization, indicating the transformation to metastable aragonite and stable calcites were in progress (Figure 4d). After 60 mins crystallization, particles with cauliflower-shaped spherical aggregates, bouquet-like and dumbbell-like needles, and cubic bulks can be observed (Figure 4e).

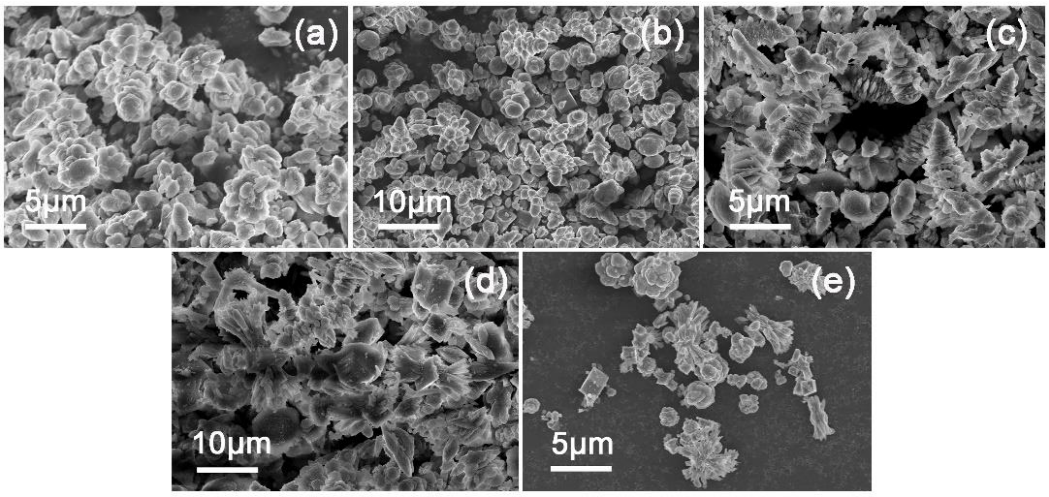

Figure 4. SEM images of $CaCO_3$ crystals in kerosene emulsion with various reaction times (5 mins, 10 mins, 20 mins, 30 mins, and 60 mins).

For gaining an insight into the influence of reaction temperature on the crystallization of $CaCO_3$ in this unique system, thus, the morphological change of precipitated particles as a function a temperature were shown in Figure 5. Specifically, when the reaction temperature was 35°C, the particles were sphere-aggregated with a diameter about 6μm (Figure 5a), whereas when the reaction temperature increased to 45°C, the precipitated particles presented in the form of cubic-like, dumbbell-shaped and sphere-aggregated with irregular size (Figure 5b). While at 55°C, a large number of disordered products formed (Figure 5c). Following, the morphology of these particles presented need-like and bundle-like (Figure 5d–f) with increasing temperature (65°C, 75°C, 85°C). Moreover, a mixture of vaterite and calcite were obtained at 35°C, and as the reaction temperature increased higher than 45°C, the aragonite phase emerged. XRD spectra of various $CaCO_3$ samples corroborated the FTIR results, the fraction of aragonite increased progressively with reaction temperature increased, and the proportion of calcite fluctuated at about 40% (Figures S2 and S3).

Preprints (www.preprints.org) | NOT PEER-REVIEWED | Posted: 25 April 2023 doi:10.20944/preprints202304.0888.v1

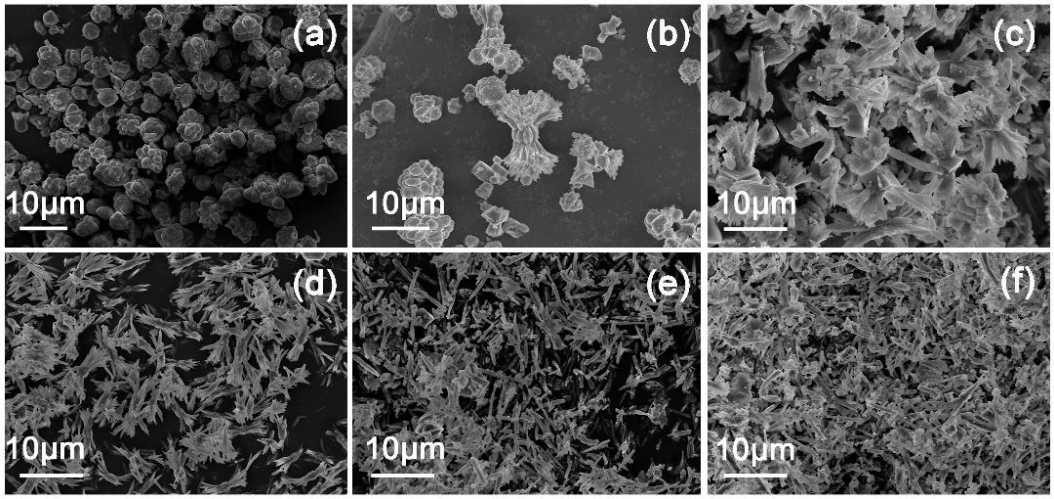

Figure 5. SEM images of $CaCO_3$ crystals in kerosene emulsion with various reaction temperatures ((**a**–**f**) 35 °C, 45 °C, 55 °C, 65 °C, 75 °C, and 85 °C).

3.3. Growth mechansim of the polymorphic symbiotic mixed $CaCO_3$ crystals

The mineralization of $CaCO_3$ under general conditions prefer to form metastable ACC first, and then transform to crystalline phase vaterite, aragonite and calcite [30]. On the basis of the above-mentioned investigations, the formation mechanism can be identified as four steps: mixing of CO_3^{2-} and HABS molecules; pre-nucleation stage (containing the formation of ion pairs and pre-nucleation clusters); nucleation stage (nucleation of ACC-I and ACC-II); post-nucleation stage (crystallization of vaterite, aragonite and calcite) (Figure 6) [31,32].

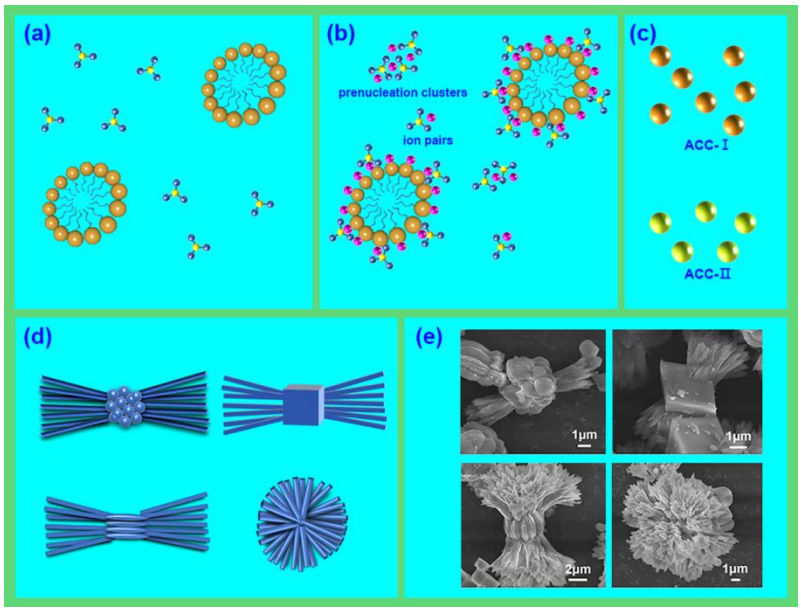

Figure 6. Proposed growth mechanisms of $CaCO_3$ in HABS/kerosene emulsion.

A schematic landscape of the mechanism of $CaCO_3$ in the HABS/kerosene emulsion is shown in Figure 6. The HABS stabilized micelles acted as a framework for the mineralization of $CaCO_3$, and then lots of Ca^{2+} were associated with the sulfonate groups via electrostatic interaction, generating pre-nucleation clusters and partial ion pairs. Following, the sequential nucleation of ACC interconnected with HABS molecules. Finally, these nanoparticles transformed into micro-meter crystals by a "dissolution-reprecipitation mechanism", forming the soft symbiotic aragonite particles that made of HABS scaffold and a small quantity of kerosene matrix.

Preprints (www.preprints.org) | NOT PEER-REVIEWED | Posted: 25 April 2023 doi:10.20944/preprints202304.0888.v1

4. Conclusions

In summary, aragonite based symbiotic mixed $CaCO_3$ crystals with superstructures were obtained in HABS/ kerosene O/W emulsion. It is found that HABS has a stabilizing effect on metastable $CaCO_3$ phases and the interface between kerosene and water. There is a synergistic effect between HABS and kerosene phase, giving assistance to the formation of $CaCO_3$ with special morphology, such as rosette-like, bouquet-like and dumbbell-like superstructures. This work explained how anionic surfactant HABS regulate the crystallization of $CaCO_3$ systemically in O/W emulsion system, made a clear insight on that HABS can be industrially used to prevent $CaCO_3$ from hard calcite scaling, and also provided a novel strategy for organic-inorganic composites manufacturing.

Supplementary Materials: The following supporting information can be downloaded at the website of this paper posted on Preprints.org.

Author Contributions: Conceptualization, methodology, investigation, writing original draft, W.H.; formal analysis, data curation, investigation, J.H., W.S., J.L. and H.G.; methodology, resources, validation, C.Z., Q.W., X.L. and M.C.; conceptualization, funding acquisition, project administration, supervision, writing-review & editing, W.S. All authors have read and agreed to the published version of the manuscript.

Funding: This work was financial supported by National Natural Science Foundation of China (#51404069) and State Key Laboratory Opening Project Foundation of Jilin University (#2018-16).

Data Availability Statement: Data can be made available upon request from the corresponding author.

Acknowledgments: We are grateful to the group of Xiaoyang Liu (State Key Laboratory of Inorganic Synthesis and Preparative Chemistry, College of Chemistry, Jilin University) and microscopic test center of the Northeast Petroleum University for characterization.

Conflicts of Interest: The authors declare no conflict of interest.

References

1. Liu, Z.; Shao, C.; Jin, B.; Zhang, Z.; Zhao, Y.; Xu, X.; Tang, R. Crosslinking ionic oligomers as conformable precursors to calcium carbonate. *Nature* **2019**, *574*, 394–398.
2. Zhang, A.; Xiao, Z.; Liu, Q.; Li, P.; Xu, F.; Liu, J.; Tao, H.; Feng, Li.; Song, S.; Liu, Z.; Huang, G. $CaCO_3$-Encapuslated Microspheres for Enhanced Transhepatic Arterial Embolization Treatment of Hepatocellular Carcinoma. *Adv. Healthc. Mater.* **2021**, *10*, 2100748.
3. Feng, Z.; Yang, T.; Liang, T.; Wu, Z.; Wu, T.; Zhang, J.; Yu, L. Biomineralization of calcium carbonate under amino acid carbon dots and its application in bioimaging. *Mater. Design.* **2022**, *217*, 110644.
4. Liu, Z.; Zhang, Z.; Wang, Z.; Jin, B.; Li, D.; Tao, J.; Tang, R.; De Yoreo, J. J. Shape-preserving amorphous-to-crystalline transformation of $CaCO_3$ revealed by in situ TEM. *P. Natl. Acad. Sci.* **2020**, *117*, 3397-3404.
5. Politi,Y.; Arad, T.; Klein, E.; Weiner, S.; Addadi, L. Sea Urchin Spine Calcite Forms via a Transient Amorphous Calcium Carbonate Phase. *Science* **2004**, *306*, 1161-1164.
6. Liu, R.; Liu, F.; Zhao, S.; Su, Y.; Wang, D.; Shen, Q. Crystallization and oriented attachment of monohydrocalcite and its crystalline phase transformatio. *CrystEngComm* **2013**, *15*, 509-515.
7. Rodríguez-Ruiz, I.; Veesler, S.; Gómez-Morales, J.; Delgado-Lopez, J. M.; Grauby, O.; Hammadi, Z.; Candoni, N.; García-Ruiz, J. M. Transient Calcium Carbonate Hexahydrate (Ikaite) Nucleated and Stabilized in Confined Nano- and Picovolumes. *Cryst. Growth Des.* **2014**, *14*, 792-802.
8. Liu, X.; Wang, Y.; Ma, Z.; Zhou, W.; Wang, X.; Zhou, H.; Wang, X.; Wang, J.; Shi, W. HABS-Silicate Controlled Synthesis of Worm-Like Calcite via Orientated Attachment. *ChemistrySelect* **2021**, *6*, 1199-1203.
9. Pokroy, B.; Zolotoyabko, E. Aragonite growth on single-crystal substrates displaying a threefold axis. *Chem. Commun.* **2005**, *16*, 2140-2142.
10. Shi, W.; Ma, Z.; Mu, Y.; Wang, J.; Liu, X.; Dong, Z.; Wang, S.; Bai, M.; Teng, Z. Interfacial self-propagation of oleophilic vaterite in crude oil emulsion and its application for reinforcing polyethylene. *Powder Technol.* **2020**, *363*, 642-651.
11. Zou, Z.; Habraken, W. J. E. M.; Matveeva, G.; Jensen, A. C. S.; Bertinetti, L.; Hood, M. A.; Sun, C.; Gilbert, P. U. P. A.; Polishchuk, I.; Pokroy, B.; Mahamid, J.; Politi, Y.; Weiner, S.; Werner, P.; Bette, S.; Dinnebier, R.;

Preprints (www.preprints.org) | NOT PEER-REVIEWED | Posted: 25 April 2023 doi:10.20944/preprints202304.0888.v1

Kolb, U.; Zolotoyabko, E.; Fratzl, P. A hydrated crystalline calcium carbonate phase: Calcium carbonate hemihydrate. *Science* **2019**, *363*, 396-400.

12. Li, Y.-X.; Jiang, Y. Synergistic Occlusion of Doxorubicin and Hydrogels in $CaCO_3$ Composites for Controlled Drug Release. *Crystals* **2023**, *13*, 132 .
13. Ueno, Y.; Futagawa, H.; Takagi, Y.; Ueno, A.; Mizushima, Y. Drug-incorporating calcium carbonate nanoparticles for a new delivery system. *J. Control. Release.* **2005**, *103*, 93-98.
14. Sheng, K.; Ge, H.; Huang, X.; Zhang, Y.; Song, Y.; Ge, F.; Zhao, Y.; Meng, X. Formation and inhibition of calcium carbonate crystals under cathodic polarization conditions. *Crystals* **2020**, *10*, 275.
15. Balthasar, U.; Cusack, M. Aragonite-calcite seas—quantifying the gray area. Geology 2015, 43, 99-102.
16. Robles-Fernández, A.; Areias, C.; Daffonchio, D.; Vahrenkamp, V.C.; Sánchez-Román, M. The role of microorganisms in the nucleation of carbonates, environmental implications and applications. *Minerals* **2022**, *12*, 1562.
17. Li, M.; Lebeau, B.; Mann, S. Synthesis of Aragonite Nanofilament Networks by Mesoscale Self-Assembly and Transformation in Reverse Microemulsions. *Adv. Mater.* **2003**, *15*, 2032-2035.
18. Zhou, G. T.; Yao, Q. Z.; Ni, J.; Jin, G. Formation of aragonite mesocrystals and implication for biomineralization. *Am. Mineral.* **2009**, *94*, 293-302.
19. Fermani, S.; Džakula, B.N.; Reggi, M.; Falini, G.; Kralj, D. Effects of magnesium and temperature control on aragonite crystal aggregation and morphology. *CrystEngComm* **2017**, *19*, 2451-2455.
20. Yang, L.; Chu, D.; Sun, H.; Ge, G. Room temperature synthesis of flower-like $CaCO_3$ architectures**.** *New J. Chem.* **2016**, *40*, 571-577.
21. Ma, Z.; Mu, Y.; Shi, W.; Wang, J.; Liu, X.; Wang, X.; Dong, Z. HPAM–HABS induced synthesis of a labyrinth-like surface of calcite *via* rhombohedral lattice growth from the nanoscale. *CrystEngComm* **2018**, *20*, 3445-3448.
22. Lai, Y.; Chen, L.; Bao, W. Glycine-mediated, selective preparation of monodisperse spherical vaterite calcium carbonate in various reaction systems. *Cryst. Growth Des.* **2015**, *15*, 1194–1200.
23. Park, H. K.; Lee, I.; Kim, K. Controlled growth of calcium carbonate by poly(ethylenimine) at the air/water interface. *Chem. Commun.* **2004**, *1*, 24-25.
24. Rodriguez-Blanco, J. D.; Shaw, S.; Benning, L. G. The kinetics and mechanisms of amorphous calcium carbonate (ACC) crystallization to calcite, *via*vaterite. *Nanoscale* **2011**, *3*, 265-271.
25. Zheng, L.; Hu, Y.; Ma, Y.; Zhou, Y.; Nie, F.; Liu, X.; Pei, C. Egg-white-mediated crystallization of calcium carbonate. *J. Cryst. Growth.* **2012**, *361*, 217-224.
26. Guo, B.; Zhao, T.; Sha, F.; Zhang, F.; Li, Q.; Zhang, J. Control over crystallization of $CaCO_3$ micro-particles by a novel CO_2SM. *CrystEngComm* **2015**, *17*, 7896-7904.
27. Shi, W.; Ma, Z.; Wang, Y.; Wang, J.; Li, B.; Wang, X.; Zhou, W.; Cheng, J. HPAM assisted controllable synthesis of peanut-like $CaCO_3$ in fixed silicate solution. *Colloid. Surface. A.* **2017**, *535*, 34-40.
28. Dai, Y.; Zou, H.; Zhu, H.; Zhou, X.; Song, Y.; Shi, Z.; Sheng, Y. Controlled synthesis of calcite/vaterite/aragonite and their applications as red phosphors doped with Eu^{3+} ions. *CrystEngComm* **2017**, *19*, 2758-2767.
29. Sarkar, A.; Dutta, K.; Mahapatra, S. Polymorph Control of Calcium Carbonate Using Insoluble Layered Double Hydroxide. *Cryst. Growth Des*. **2013**, *13*, 204-211.
30. Porras, M.; Solans, C.; González, C.; Gutiérreza, J. M. Properties of water-in-oil (W/O) nano-emulsions prepared by a low-energy emulsification method. *Colloid. Surface. A.* **2008**, *324*, 181-188.
31. Bots, P.; Benning, L. G.; Rodriguez-Blanco, J. D.; Roncal-Herrero, T.; Shaw, S. Mechanistic Insights into the Crystallization of Amorphous Calcium Carbonate (ACC). *Cryst. Growth Des.* **2012**, *12*, 3806-3814.
32. Farhadi-Khouzani, M.; Chevrier, D. M.; Zhang, P.; Hedin, N.; Gebauer, D. Water as the key to proto-aragonite amorphous $CaCO_3$. *Angew. Chem. Int. Edit.* **2016**, *55*, 8117-8120.
33. Gebauer, D.; Kellermeier, M.; Gale, J. D.; Bergström, L.; Cölfen, H. Pre-nucleation clusters as solute precursors in crystallisation. *Chem. Soc. Rev.* **2014**, *43*, 2348-2371.

Disclaimer/Publisher's Note: The statements, opinions and data contained in all publications are solely those of the individual author(s) and contributor(s) and not of MDPI and/or the editor(s). MDPI and/or the editor(s) disclaim responsibility for any injury to people or property resulting from any ideas, methods, instructions or products referred to in the content.